INTENSITY INTERFEROMETER TO MEASURE
BUNCH LENGTH AT SPEAR3[*]

J. Corbett, SLAC National Accelerator Laboratory, Menlo Park, USA
T. Mitsuhashi, KEK, Tsukuba, Japan

Abstract

The electron bunch length in a storage ring can be measured using a streak camera, electro-optics or non-linear pulse correlation with a range of system complexity and cost. An alternative method is to use 2th-order 'intensity interferometry'. In this configuration, spatially filtered monochromatic SR light is split, delayed, recombined and discrete photons detected with photomultipliers. A coincidence detector records two-photon arrival events. As one arm of the interferometer is scanned, interference events within the radiation coherence time can reduce the coincidence rate to reveal the electron bunch length. In this paper we review the intensity interferometer and report on the system at SPEAR3.

INTRODUCTION

SPEAR3 currently provides laser pump, x-ray probe measurement capability complementary to the SLAC LCLS and UED programs. Although the x-ray pulse length is of order 20ps rms, meaningful ultrafast research is possible [1] with efforts underway to produce shorter pulses in the few ps range [2-6]. At these pulse lengths, vacuum chamber impedance and coherent synchrotron radiation (CSR) limit the bunch charge creating unique challenges for both the User community and beam diagnostics.

In particular, the bunch length can be difficult to measure when narrow-band filtering creates low optical photon flux. Synchronized measurements such as streak camera, laser cross-correlation [7,8] or electro-optic techniques [9] are further complicated by the presence of synchrotron oscillations. Auto-correlation [10] and fluctuation analysis [11] are less sensitive to synchrotron oscillations but have limited signal/noise ratio at low bunch charge. In this paper we revisit the 2-photon intensity interferometer first developed at the University of Tokyo [12] and later applied to measure bunch length at the Photon Factory [10].

Intensity interferometry is effective for visible SR pulse measurements on a storage ring because the light is incoherent and the system is insensitive to synchrotron oscillations, air turbulence and low-amplitude vibrations. The method is particularly effective for weak light, short pulse applications where the coherence time of the field is comparable to the pulse duration time.

OPTICAL INTERFEROMETRY

Optical interferometers appear in a variety of configurations and are used for many applications. Some use fringe counts while others depend on the statistical correlation of field amplitudes in space and/or time by relying the inference contrast $\Gamma^{(1)}(\mathbf{r_1},\mathbf{r_2},t_1,t_2) = <E_1(\mathbf{r_1},t_1) E_2(\mathbf{r_2},t_2)>$. For ergodic light the averaging can be taken over a statistical ensemble or a finite measurement interval [13]. By extension, higher order coherence functions are also possible [14], most commonly fourth-order correlation $\Gamma^{(2)}=<E_1E_2E_3E_4>$. For random field emission processes where the light is modelled as statistically Gaussian, $\Gamma^{(n)}$ can be characterized by moments of the Gaussian distribution.

Second Order Interferometry

In the spatial domain, second-order interferometry can be used to resolve the size of an incoherent emission source. In a famous example, Michelson combined the fields from two spatially-separated rays of starlight at Mt. Wilson to produce interference fringes with finite contrast [15]. The contrast is mathematically represented in the 2nd-order correlation term $<E_1E_2>$. Michelson's second-order stellar interferometer revealed the angular diameter of nearby red giant α -Orionis to be φ ~ 0.047" and have a diameter ~ 300 times larger than our sun.

About 10 years later, Van Cittert [16] and Zernike [17] formalized the theoretical basis by demonstrating that under sufficiently paraxial conditions the fringe contrast and source distribution form a Fourier-transform pair. As suggested by Goodman, the Van Cittert-Zernike relation 'is undoubtedly one of the most important theorems of modern optics' [14]. In a landmark development for accelerator diagnostics, the stellar interferometer concept was applied to visible SR light to measure transverse electron beam size at the Photon Factory [18].

An example of second-order _temporal_ interferometry came again from Michelson in the search for electromagnetic aether, Fig. 1 [19]. In this configuration, the fields from the two arms of a amplitude dividing interferometer were recombined to form a fringe pattern with phase dependent on the time delay.
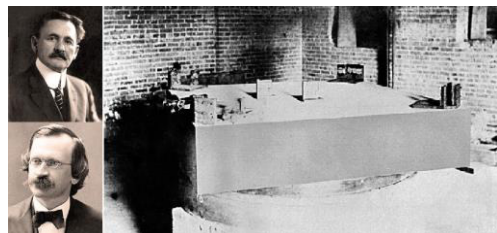

Figure 1: The Michelson-Morley interferometer.

INTENSITY CORRELATION

The angular resolution of Michelson's stellar stellar interferometer was inherently limited by mechanical vibrations and air turbulence which placed an upper bound on pinhole separation. A breakthrough occurred in the 1950's when Hanbury Brown and Twiss (HBT) demonstrated electronic correlation of optical intensity fluctuations at much longer receiver baselines. With the new device they were able to resolve the angular distribution of Sirius to be 0.0063" using visible light [20]. The new method of '2th-order intensity correlation' ignited widespread debate and ultimately launched the field of quantum optics led by Roy Glauber [21] and collaborators.

As seen in Fig. 2, the HBT approach can also be used to study the temporal coherence of narrow-band thermal light [22]. Similar to the measurement of stellar diameters, time-domain intensity correlation is based on evaluation of the quantity $\langle I(t)I(t+\tau)\rangle$ with measurement resolution determined by detector response time relative to the characteristic fluctuation times in the optical field.
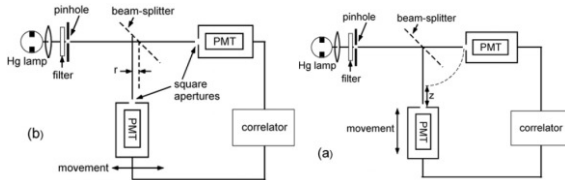
Figure 2: HBT spatial and temporal intensity

INTENSITY INTERFEROMETRY

Intensity interferometry works in the discrete photon detection mode to record 4th-order field correlations using two arms of an optical interferometer. In an early demonstration, Ou, et al. measured the field coherence time τ_c in CW thermal light, well below the photoelectric detector response time [23]. Soon after, Miyamoto, et al. extended the work to measure both the field coherence time and the pulse duration in a train of optical pulses [12]. Recognizing the application, Mitsuhashi constructed a similar system at the Photon Factory to measure the electron bunch length using incoherent visible SR light [10]. The KEK optical system was then shipped to SLAC for tests at SPEAR3.

To understand the mechanics of an intensity interferometer, first consider the path of an incoming optical pulse. As illustrated in Fig. 3, a 50:50 beam splitter (BS) first divides the field energy equally into two arms of the interferometer. As the length of one arm is scanned, the pulse is effectively convolved with itself as it recombines at the interaction point. In order to measure the pulse overlap integral, a physical reaction is required with sufficient cross-section to generate a measureable signal. In this case, the 'reaction' is a 2-photon, 4th-order field correlation.

At the interaction point, field energy from Arm A can propagate to detectors D1 and D2, and similarly for Arm B. Taking into account the 90° phase shift on reflection at
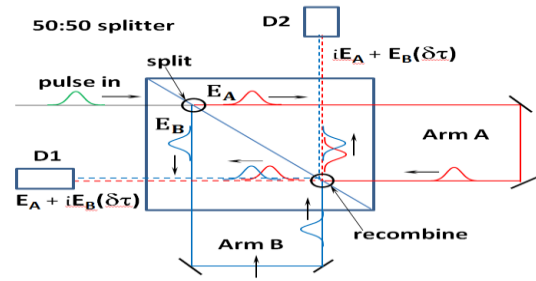
Figure 3: The two-photon intensity interferometer.

the BS [24], the fields at detectors D1 and D2 can be written

$$E_1(\delta\tau) = E_A + iE_B(\delta\tau) \qquad [1a]$$

$$E_2(\delta\tau) = iE_A + E_B(\delta\tau) \qquad [1b]$$

where E_A and E_B are defined in Fig. 3 and $\delta\tau$ is the differential time-of-flight in Arm B. The corresponding measurable intensities at D1 and D2 are

$$I_1(\delta\tau) = E_1 E_1^* = (E_A + iE_B(\delta\tau))(E_A + iE_B(\delta\tau))^* \quad [2a]$$

$$I_2(\delta\tau) = E_2 E_2^* = (iE_A + E_B(\delta\tau))(iE_A + E_B(\delta\tau))^* \quad [2b]$$

In practice detectors D1 and D2 are photomultiplier tubes (PMT) operating in discrete-photon detection mode. The PMT electronics produce a TTL pulse for each detected event. A coincidence detector multiplies the output of D1 with D2 to generate a 'count' C_{12} when two detector events overlap in time. Electronically, a count is recorded when both I_1 and I_2 are logically true. Two photons must enter the interferometer within the 10 ns PMT pulse time duration to generate a count.

From Eq. 2, the count rate $C_{12} = I_1 I_2$ is 4th-order in field and contains a total of sixteen 4th-order terms each depending on the relative time delay $\delta\tau$ in the interferometer. Multiplying out the expression for $I_1 I_2$, 8 terms are pure imaginary (not observable), 4 terms are positive real and 4 terms are negative real. Physically the negative real terms represent 2-photon interference and reduce the count rate.

Referring again to Fig. 3, as the length of Arm B is scanned, the positive real terms generate a constant 'background' signal of coincidence events. The negative real terms occur when fields E_A and E_B arrive at the beamsplitter interface within a coherence time of the light, τ_c. The probability for two photons to arrive within a coherence time is highest when the path length through both two arms is equal (maximum pulse overlap), and less when the path differential is non-zero.

In practice, the count rate must integrated over both the detector response time and the total measurement time. For a Gaussian SR pulse duration with random Gaussian field emission statistics having characteristic coherence time τ_c, the double integral evaluates to [10,12,23]

$$C_{12}(\delta\tau) = K\left(1 + \frac{\tau^*}{\tau_p}\left[1 - \frac{1}{2}exp\left(-\frac{\delta\tau^2}{4\tau_p^2}\right)\right]\right) \qquad [4]$$

where a term representing direct correlation between wavepackets has been supressed [10], τ_p is the rms pulse duration, K is a normalization coefficient and

$$\frac{1}{\tau^{*2}} = \frac{1}{\tau_p^2} + \frac{1}{\tau_c^2} \sim \frac{1}{\tau_c^2} \quad for\ \tau_p \gg \tau_c\ . \qquad [5]$$

By inspection, the negative exponential term in Eq. 4 causes a 'dip' in the coincidence count during the interferometer scan, with a depth equal to $\frac{\tau^*}{2\tau_p} \sim \frac{\tau_c}{2\tau_p}$.

EXPERIMENTAL APPARATUS

Before entering the intensity interferometer, the unfocused visible SR beam is first condensed by a factor of ~ 10 with telescope optics to increase count rate. A microscope objective then focuses the beam through a ~4μm pinhole to produce a pure Gaussian spatial mode. Next the beam is collimated and passes through a beam polarizer to select the π or σ SR polarization mode. The collimating lens is adjusted to maintain a constant beam cross-section throughout interferometer for optimal pulse overlap during the interferometer scan.

Finally, before entering the beam splitter, the SR light passes through a narrow bandpass filter (BPF) with center wavelength λ=632.8 nm and an adjustable iris to define collimation diameter. After the BPF, the beam intensity is ~10^4 cps at the photomultipliers, or about 1 photon detected every 100 turns. In order to eliminate coincident events between bunches, measurements are made with bunch separations longer than the 10ns PMT response time. Shielding is important throughout the system to avoid spurious PMT counts. Typical coincidence count rates are of order 10^2 cps for PMT count rates of 10^4 cps.

By inspection, the exponential term in Eq. 4 causes the 'dip' in the coincidence count rate during the interferometer scan with a depth of $\frac{\tau^*}{2\tau_p} \sim \frac{\tau_c}{2\tau_p}$. Referring to Table 1, the anticipated interference dip is about 3% for a 20 ps rms bunch length. A plot of the expected interference pattern for several values of τ_p is shown in Fig. 4. Bunch lengths of τ_p=3 ps and 10 ps are possible in low-alpha mode [2] while τ_p=30 ps corresponds to a bunch with ~ 25 ma beam current [25]. In the future shorter bunches are envisioned using fast vertical deflection techniques [3-6].

Table 1: Optical Parameters Pertaining to Interference dip

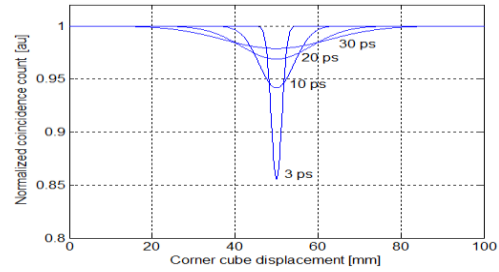| parameter	symbol	value
bunch length	τ_p, l_p	20 ps, 6 mm
bandpass	λ, $\Delta\lambda$	632.8 nm, 1 nm
coherence $\left(\frac{\lambda^2}{\Delta\lambda}\right)$	τ_c, l_c	399 μm, 1.3 ps
$\frac{\tau_c}{2\tau_p}$	dip	3.1%

Figure 4: Calculated interference pattern for electron bunch length τ_p = 3, 10, 20 and 30 ps rms. τ_c = 1.3 ps.

At this time the interference dip has not been detected at SPEAR3 and the cause is not certain. Candidate sources of error are the linearity of the Arm B rail scan impacting optical alignment, bandpass filter quality, masking of background signal, electronics used for NIM/TTL signal conversion and the coincidence detection electronics. A plot of an interferogram measured at the Photon Factory at KEK is shown in Fig. 5.
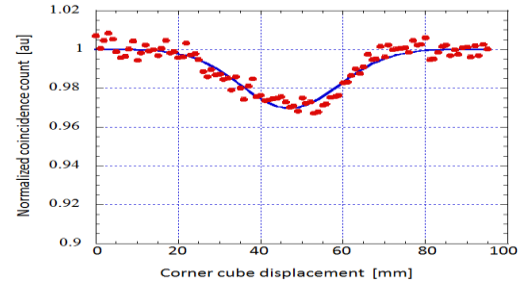

Figure 5: Intensity interferogram at the KEK Photon Factory. Pulse length 16.8 ps rms. τ_c = 1.3 ps.

SUMMARY

The KEK intensity interferometer is currently installed at SPEAR3 for bunch length measurements. The system is well suited for weak, incoherent SR light in the visible regime. In the short pulse regime below the streak camera resolution limit, the contrast in 4th-order field interference is expected to decrease well below 10% .

ACKNOWLEDGMENTS

REFERENCES

[1] M. Kozina *et al.*, "Transient Atomic Displacements in Thin Films with Picosecond and Femtometer Resolution", Structural Dynamics 1, 034301 (2014).

[2] X. Huang, "Low alpha mode for SPEAR3", PAC07, Albuquerque, NM, (2007).

[3] X. Huang, T. Rabedeau and J. Safranek, "Generation of Picosecond Electron Bunches in Storage Rings", JSR Vol. 21 5 (2014).

[4] X. Huang, "Short Pulse Options for SPEAR3", Internal SPEAR3 AP Note 62 (2016).

[5] J. Safranek *et al.,* "Resonant Crabbing for Short Pulses in SPEAR3", to be published.

[6] K. Bane *et al*., "Generation of Short Pulses in SPEAR3 with Two-frequency Crab Cavities", SSRL Internal Report, February, 2017.

[7] M. Zolotorev *et al*., "Development of a Longitudinal Density Monitor for Storage Rings", PAC03, Portland, Oregon (2003).

[8] T. Miller *et al.*, "Bunch Length Measurements with Laser/SR Cross-correlation", IPAC10, Kyoto, Japan (2010).

[9] N. Hiller, "Electro-Optical Bunch Length Measurements at the ANKA Storage Ring", PhD Thesis, Karlsruhe Institute of Technology (KIT), (2013).

[10] T. Mitsuhashi, "Measurement of Bunch Length using Intensity Interferometry", EPAC2002, Paris, France.

[11] F. Sannibale *et al*., "Absolute Bunch Length Measurements at the ALS by Incoherent SR Fluctuation Analysis", IPAC2007, Albuquerque, NM (2007).

[12] Y. Miyamoto *et al*., "Measurement of Ultrafast Optical Pulses with Two-photon Interference", Optics Letters, 18, 11 (1993).

[13] L. Mandel and E. Wolf , "Optical Coherence and Quantum Optics", Cambridge University Press (1995).

[14] J.Goodman, "Statistical Optics", Wiley & Sons (1985).

[15] A.A. Michelson and F.G. Pease, "Measurement of the Diameter of α-Orionis with the Interferometer", Astrophysical Journal, 249-258 (1921).

[16] P.H. Van-Cittert, Physica 1, 2001 (1934).

[17] F.Zernike, "The Concept of Degree of Coherence and Application to Optical Problems", Physica, 5 (1938).

[18] T. Mitsuhashi, "Beam Profile and Size Measurements by SR Interferometers", in Beam Measurements, Joint US-CERN-Japan-Russia School, Montreaux, Switzerland, World Scientific (1998).

[19] A. Michelson, "The Relative Motion of the Earth and the Luminiferous Aether", Amer. Journal Sci. 22 (1881).

[20] Hanbury Brown and Twiss, "A Test of a New Type of Stellar Interferometer on Sirius", Nature 178 (1956).

[21] R. Glauber, "The Quantum Theory of Optical Coherence", Physical Review 130, 6 (1963). 2005 Nobel prize citation, 'for his contribution to the quantum theory of optical coherence'.

[22] Hanbury Brown and Twiss, "Correlation between Photons in Two Coherent Beams of Light", Nature 177 (1956).

[23] Z.Y.Ou *et al*., "Fourth-order Interference Technique for Determining the Coherence Time of a Light Beam", J. Opt. Soc. Am. B, 6, 1 (1989).

[24] Z.Y. Ou *et al.*, "Relation between Input and Output States for a Beam Splitter", Optics Comm. 63, 2 (1987).

[25] J. Corbett, W. Cheng and X. Huang, "Short Bunch Measurements in SPEAR3", PAC09, Vancouver, Canada (2009).